Acta Crystallographica Section F
**Structural Biology Communications**
ISSN 2053-230X

# Crystallization and preliminary X-ray crystallographic analysis of the catalytic domain of membrane type 1 matrix metalloproteinase

**Hideaki Ogata,[a]* Elena Decaneto,[a,b] Moran Grossman,[b,c] Martina Havenith,[b] Irit Sagi,[c] Wolfgang Lubitz[a] and Markus Knipp[a,b]***

[a]Max-Planck-Institut für Chemische Energiekonversion, Stiftstrasse 34-36, 45470 Mülheim an der Ruhr, Germany, [b]Physikalische Chemie II, Ruhr-Universität Bochum, Universitätsstrasse 150, 44801 Bochum, Germany, and [c]Department of Biological Regulation, The Weizmann Institute of Science, Rehovot 76100, Israel

Correspondence e-mail: hideaki.ogata@cec.mpg.de, markus.knipp@cec.mpg.de

Received 2 December 2013
Accepted 30 December 2013

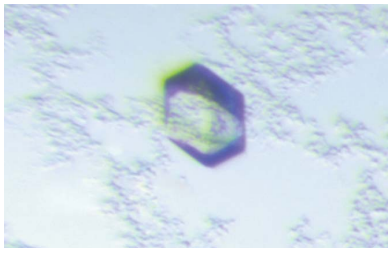



Membrane type 1 matrix metalloproteinase (MT1-MMP) belongs to the large family of zinc-dependent endopeptidases termed MMPs that are located in the extracellular matrix. MT1-MMP was crystallized at 277 K using the vapour-diffusion method with PEG as a precipitating agent. Data sets for MT1-MMP were collected to 2.24 Å resolution at 100 K. The crystals belonged to space group $P4_32_12$, with unit-cell parameters $a$ = 62.99, $c$ = 122.60 Å. The crystal contained one molecule per asymmetric unit, with a Matthews coefficient ($V_M$) of 2.90 Å$^3$ Da$^{-1}$; the solvent content is estimated to be 57.6%.

## 1. Introduction

Matrix metalloproteinases (MMPs) comprise a family of zinc-dependent endopeptidases found in the extracellular matrix (Tallant *et al.*, 2010; Murphy & Nagase, 2008). They play a major role in the degradation of extracellular matrix substrates such as collagens, gelatin, fibronectin and others during embryogenesis, wound healing, bone resorption *etc.* (Vargová *et al.*, 2012). More than 20 members of the MMP family are expressed in the human organism, many of which have been associated with common diseases such as atherosclerosis, arthritis, tumourigenesis, cancer and neuronal pathologies (Tallant *et al.*, 2010; Murphy & Nagase, 2008). Therefore, researchers worldwide have been trying to find specific peptide-based inhibitors or other low-molecular-weight inhibitors for pharmaceutical application (Gupta & Patil, 2012; Ndinguri *et al.*, 2012). However, the degree of specificity required for pharmaceutical use has not yet been obtained. It is now believed that specificity is not primarily obtained *via* the recognition of target peptides by the active-site cleft but through multiple interfacial interactions between a target substrate protein and the MMP (Murphy & Nagase, 2008; Udi *et al.*, 2013). This hypothesis is supported by the fact that native MMP inhibitors, for example tissue inhibitors of metalloproteinases (TIMP), are also proteins, which allow interaction specificity to be gained through multiple surface–surface interactions (Murphy & Nagase, 2008; Grossman *et al.*, 2010).

Upon expression, the MMPs contain an N-terminal pro-domain motif, which inhibits protein activity through binding of a pro-domain Cys to the active-site $Zn^{2+}$ (Tallant *et al.*, 2010; Nagase & Woessner, 1999; Vargová *et al.*, 2012). Zymogenic activation of the enzyme allows the substrate peptides to enter the active site for metal-catalyzed hydrolysis. Besides the active-site $Zn^{2+}$, MMPs contain a second $Zn^{2+}$-binding site and two $Ca^{2+}$-binding sites of unknown function. The catalytic domain downstream of the pro-domain is linked to a haemopexin-like domain *via* the so-called hinge region in most MMPs (Nagase & Woessner, 1999). The purpose of the haemopexin-like domains is not clear, but they may be important for substrate recognition and enzyme regulation. A group of MMPs, including MMP-14 to MMP-17, MMP-24 and MMP-25, are membrane-anchored proteins, with MMP-14 to MMP-16 and MMP-24 having an integral membrane-spanning domain located C-terminal to the haemopexin-like domain. These proteins are termed MT-MMPs, where MMP-14 is specifically named MT1-MMP.

Of the 168 X-ray structures of MMP catalytic domains currently available from the PDB, only MMP-1 (PDB entry 3shi; Bertini *et al.*, 2012), MMP-2 (gelatinase A; PDB entry 1qib; Dhanaraj *et al.*, 1999), MMP-3 (stromelysin; PDB entries 1qia and 1qic; Pavlovsky *et al.*, 1999), MMP-8 (PDB entry 2oy4; Bertini *et al.*, 2006) and MMP-12 (PDB entry 2oxu; Bertini *et al.*, 2006) were crystallized in the uninhibited form, with only the crystals of MMP-1, MMP-8 and MMP-12 diffracting to a resolution of <2.5 Å. Detailed structural knowledge of the catalytic domains in all stages of the enzymatic activity is indispensable for understanding the catalytic process and thus the controlled manipulation of the enzymatic activity. The structure of the catalytic domain of none of the membrane-associated MMPs has been solved to date except for MT1-MMP in complex with TIMP-2 (PDB entries 1buv and 1bqq; Fernandez-Catalan *et al.*, 1998) and in complex with a mutant of TIMP-1 (PDB entry 3ma2; Grossman *et al.*, 2010). Here, we report the crystallization and diffraction of the uninhibited catalytic domain of human MT1-MMP.

## 2. Materials and methods

### 2.1. Purification

The plasmid containing the catalytic domain of human MT1-MMP together with the hinge linker to the haemopexin-like domain (residues 112–292) as described in Grossman *et al.* (2011) was transformed into *Escherichia coli* BL21 (DE3) (Novagen). Expression was carried out at 310 K in LB medium for 5 h after induction with 0.5 m*M* isopropyl *β*-D-1-thiogalactopyranoside (IPTG) at $OD_{600\ nm}$ = 0.8. Upon harvesting, the cells were sonicated on ice for five cycles of 1 min (Branson Sonifier, 70% output power, 1 s pulse duration). Inclusion bodies were harvested by centrifugation (6000*g*, 277 K, 15 min) and then subjected to extensive washing using a Potter–Elverheim homogenizer. The inclusion bodies were washed two times with 30 m*M* Tris–HCl pH 7.4, 30 m*M* NaCl, 1 m*M* EDTA, 2%(*v*/*v*) Tween 20, 5 m*M* *β*-mercaptoethanol, two times with 30 m*M* Tris–HCl pH 7.4, 500 m*M* NaCl, 1 m*M* EDTA, 5 m*M* *β*-mercaptoethanol and finally two times with 30 m*M* Tris–HCl pH 7.4, 30 m*M* NaCl, 1 m*M* EDTA, 5 m*M* *β*-mercaptoethanol. The inclusion bodies were then homogenized in 6 *M* urea, 50 m*M* Tris–HCl pH 8.5 and kept at 293 K for 2 h before ultracentrifugation (100 000*g*, 277 K, 30 min). Folding was carried out through dialysis (12–14 kDa molecular-weight cutoff) against a tenfold volume of 50 m*M* Tris–HCl pH 8.5, 100 m*M* NaCl, 10 m*M* $CaCl_2$, 10 µ*M* zinc acetate, 2 *M* urea (overnight at 293 K). The solution was then changed to 50 m*M* Tris–HCl pH 7.5, 100 m*M* NaCl, 10 m*M* $CaCl_2$, 10 µ*M* zinc acetate, 1 *M* urea (24 h at 277 K). Finally, the protein was dialyzed two times against 50 m*M* Tris–HCl pH 7.5, 100 m*M* NaCl, 5 m*M* $CaCl_2$, 1 µ*M* zinc acetate (24 h at 277 K). The solution was concentrated to 10 mg $ml^{-1}$ at 277 K using Amicon Ultra-0.5 centrifugal filter devices (10 kDa molecular-weight cutoff; Millipore) and the solution was then exchanged for zinc-free buffer. The quality of the samples was determined by SDS–PAGE.

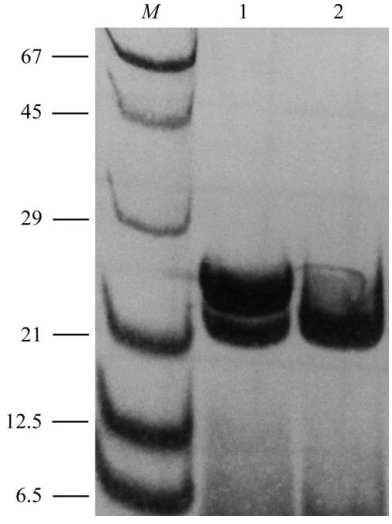


**Figure 1**
Autoproteolytic activity of MT1-MMP documented by SDS–PAGE (12%). Lane 1, recombinantly expressed human MT1-MMP catalytic domain together with the hinge region after the last dialysis step performed in 50 m*M* Tris–HCl pH 7.5, 100 m*M* NaCl, 5 m*M* $CaCl_2$, 1 µ*M* zinc acetate; lane 2, sample as in lane 1 but kept for 24 h at 293 K prior to analysis. 20 µl of the samples were incubated with 10 µl 25 m*M* Tris–HCl pH 6.8, 1 m*M* $Na_2EDTA$, 10%(*v*/*v*) glycerol, 5%(*v*/*v*) *β*-mercaptoethanol, 0.025%(*w*/*v*) bromophenol blue for 4 min at 343 K. Protein bands were stained with 0.1%(*w*/*v*) Coomassie Brilliant Blue G-250 in 10%(*v*/*v*) acetic acid and 40%(*v*/*v*) methanol. Lane *M* contains molecular-mass marker (labelled in kDa).

### 2.2. Crystallization

Screening of crystallization conditions was performed by the sitting-drop vapour-diffusion method with a Phoenix dispensing robot (Art Robbins Instruments, California, USA). The crystallization experiments consisted of 0.3 µl protein solution mixed with 0.3 µl reservoir solution and were equilibrated against 80 µl reservoir solution at 277 K. After 4–6 weeks, small crystals of MT1-MMP were obtained under several conditions from the PEG/Ion and PEG/Ion2 screening kits (Hampton Research, California, USA): (i) 0.1 *M* sodium malonate pH 4.0, 20%(*w*/*v*) PEG 3350, (ii) 4%(*v*/*v*) Tacsimate pH 6.0, 12%(*w*/*v*) PEG 3350 and (iii) 0.2 *M* ammonium nitrate, 20%(*w*/*v*) PEG 3350 pH 6.2. To obtain crystals suitable for X-ray diffraction, the crystals from condition (iii) were soaked in buffer consisting of 0.3 *M* ammonium nitrate, 25%(*w*/*v*) PEG 3350 pH 6.2 and 20%(*v*/*v*) glycerol as a cryoprotectant.

### 2.3. Data collection

Diffraction data sets were collected on beamline BL14.2 at BESSY II (Hermholtz-Zentrum Berlin, Germany). The detector was a Rayonix MX-225 (Rayonix, Illinois, USA). A complete native data set was collected to 2.24 Å resolution at an X-ray wavelength of 0.92 Å. Data collection for the Zn and Ca atoms was performed at X-ray wavelengths of 1.24 Å (zinc peak), 1.34 Å (zinc remote) and 1.95 Å (calcium). Diffraction images were indexed and integrated using the program *XDS* (Kabsch, 2010). Scaling was carried out using

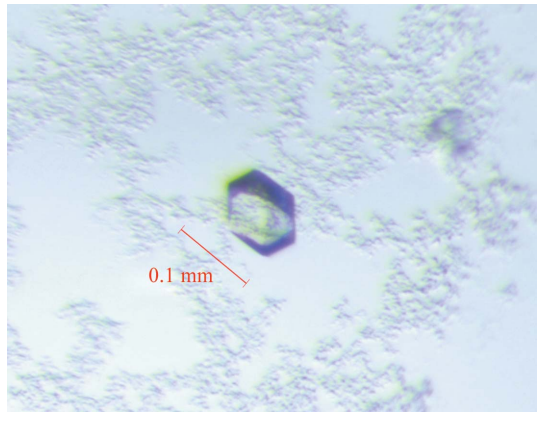


**Figure 2**
Crystals of the catalytic domain of human MT1-MMP. They were obtained after four weeks from 0.3 µl protein solution mixed with 0.3 µl reservoir solution [0.2 *M* ammonium nitrate, 20%(*w*/*v*) PEG 3350 pH 6.2] at 277 K.

*XSCALE* (Kabsch, 2010). Molecular replacement and initial refinement were carried out using *MOLREP* (Vagin & Teplyakov, 2010) and *REFMAC*5 (Murshudov *et al.*, 2011), respectively, from the *CCP*4 program package (Winn *et al.*, 2011).

## 3. Results and discussion

MT1-MMP was expressed as inclusion bodies and subsequently folded. Characterization by SDS–PAGE showed that after dialysis the protein consists of a mixture of the pure catalytic domain (apparent molecular mass 21 kDa) and a form containing the hinge region (apparent molecular mass 24 kDa) (Fig. 1). The mature protein was generated by successive autoproteolysis after 1 d at 293 K as demonstrated by SDS–PAGE (Fig. 1). The catalytic activity of the mature MT1-MMP was demonstrated by a fluorogenic assay monitoring the peptide cleavage of Mca-Lys-Pro-Leu-Gly-Leu-Lys(Dnp)-Ala-Arg-$NH_2$, where Mca is (7-methoxycoumarin-4-yl)-acetyl and Dnp is *N*-3-(2,4-dinitrophenyl)-L-2,3-diaminopropionyl (Neumann *et al.*, 2004).

MT1-MMP was crystallized at 277 K using the vapour-diffusion method with PEG as the precipitating agent. The crystal dimensions were typically 0.1 × 0.1 × 0.05 mm (Fig. 2). The crystal of MT1-MMP diffracted to 2.24 Å resolution (Fig. 3). The data-collection conditions are summarized in Table 1. The crystal belonged to space group $P4_32_12$ or $P4_12_12$. The unit-cell parameters were $a$ = 62.99, $c$ = 122.60 Å. The calculated Matthews coefficient ($V_M$; Matthews, 1968) of 2.90 Å$^3$ Da$^{-1}$, with a solvent content of 57.6%, indicates the presence of one molecule per asymmetric unit.

The molecular-replacement method was applied using the program *MOLREP*. The coordinates of the MT1-MMP–TIMP-2 complex (PDB entry 1bqq; Fernandez-Catalan *et al.*, 1998) were used as a search model. A solution of the rotation and translation parameters for one MT1-MMP molecule in space group $P4_32_12$ was obtained (the weighted $R$ factor and score were 0.518 and 0.505, respectively). In space group $P4_12_12$, the weighted $R$ factor and score were 0.574 and 0.383, respectively. Calculation of the electron-density map by molecular replacement confirmed the space group to be $P4_32_12$ with one monomer in the asymmetric unit. Zn-MAD data for calculation of the anomalous difference map were obtained from a crystal of MT1-MMP at X-ray wavelengths of 1.24 and 1.34 Å. The anomalous difference map revealed peaks that correspond to the zinc ions. Furthermore, Ca-SAD data were obtained at an X-ray wavelength of 1.95 Å, revealing peaks corresponding to calcium ions in the anomalous difference map. Model building and refinement are now in progress.

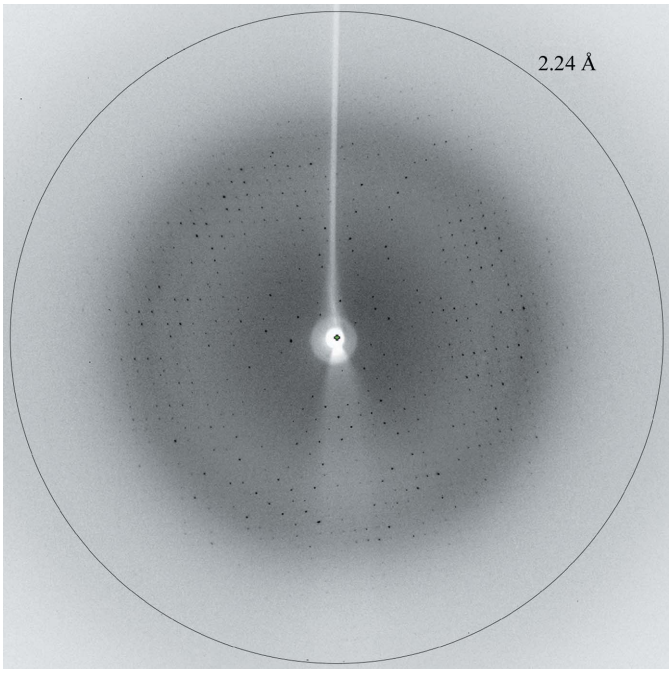


**Figure 3**
Diffraction pattern of MT1-MMP (native data). The crystal-to-detector distance was maintained at 250 mm. 100 images of 1.0° oscillation angle and 3.0 s exposure time each were collected.

**Table 1**
X-ray data-collection statistics for the catalytic domain of MT1-MMP.

Values in parentheses are for the outermost resolution shell.

| | Native | Zn peak | Zn remote | Ca peak |
|---|---|---|---|---|
| Wavelength (Å) | 0.92 | 1.24 | 1.34 | 1.95 |
| Space group | $P4_32_12$ | $P4_32_12$ | $P4_32_12$ | $P4_32_12$ |
| Unit-cell parameters | | | | |
| $a$ (Å) | 62.99 | 63.02 | 63.05 | 63.08 |
| $c$ (Å) | 122.60 | 122.64 | 122.68 | 122.79 |
| Resolution (Å) | 44.54–2.24 (2.37–2.24) | 44.56–2.46 (2.61–2.46) | 44.59–2.62 (2.78–2.62) | 44.61–2.88 (3.05–2.88) |
| No. of observed reflections | 98084 | 201819 | 161826 | 151387 |
| No. of unique reflections | 12491 | 16520 | 13552 | 10689 |
| $R_{merge}$† | 0.105 (0.998) | 0.080 (0.705) | 0.065 (0.519) | 0.163 (1.145) |
| Completeness | 0.998 (0.993) | 0.962 (0.806) | 0.952 (0.777) | 0.998 (0.989) |
| $\langle I/\sigma(I)\rangle$ | 16.8 (2.3) | 27.3 (2.3) | 31.2 (2.7) | 20.4 (1.9) |
| $CC_{1/2}$ | 99.8 (70.1) | 99.9 (68.4) | 99.9 (83.0) | 99.7 (68.4) |

† $R_{merge} = \sum_{hkl}\sum_i |I_i(hkl) - \langle I(hkl)\rangle| / \sum_{hkl}\sum_i I_i(hkl)$.

We are grateful for the technical assistance of Inge Heise, Norbert Dickmann and Yvonne Brandenburger (MPI for Chemical Energy Conversion, Mülheim, Germany). We thank the staff of beamline BL14.2 at BESSY II (Helmholtz-Zentrum Berlin, Germany) for their assistance during data collection. This work was supported by the Cluster of Excellence RESOLV (EXC 1069) funded by the Deutsche Forschungsgemeinschaft. Financial support was also obtained from the Max Planck Society.

## References

Bertini, I., Calderone, V., Cerofolini, L., Fragai, M., Geraldes, C. F. G. C., Hermann, P., Luchinat, C., Parigi, G. & Teixeira, J. M. C. (2012). *FEBS Lett.* **586**, 557–567.
Bertini, I., Calderone, V., Fragai, M., Luchinat, C., Maletta, M. & Yeo, K. J. (2006). *Angew. Chem. Int. Ed.* **45**, 7952–7955.
Dhanaraj, V., Williams, M. G., Ye, Q.-Z., Molina, F., Johnson, L. L., Ortwine, D. F., Pavlovsky, A., Rubin, J. R., Skeean, R. W., White, A. D., Humblet, C., Hupe, D. J. & Blundell, T.L. (1999). *Croat. Chem. Acta*, **72**, 575–591.
Fernandez-Catalan, C., Bode, W., Huber, R., Turk, D., Calvete, J. J., Lichte, A., Tschesche, H. & Maskos, K. (1998). *EMBO J.* **17**, 5238–5248.
Grossman, M., Born, B., Heyden, M., Tworowski, D., Fields, G. B., Sagi, I. & Havenith, M. (2011). *Nature Struct. Mol. Biol.* **18**, 1102–1108.
Grossman, M., Tworowski, D., Dym, O., Lee, M. H., Levy, Y., Murphy, G. & Sagi, I. (2010). *Biochemistry*, **49**, 6184–6192.
Gupta, S. P. & Patil, V. M. (2012). *Matrix Metalloproteinase Inhibitors*, edited by S. P. Gupta, pp. 35–56. Basel: Springer.
Kabsch, W. (2010). *Acta Cryst.* D**66**, 125–132.
Matthews, B. W. (1968). *J. Mol. Biol.* **33**, 491–497.
Murphy, G. & Nagase, H. (2008). *Mol. Aspects Med.* **29**, 290–308.
Murshudov, G. N., Skubák, P., Lebedev, A. A., Pannu, N. S., Steiner, R. A., Nicholls, R. A., Winn, M. D., Long, F. & Vagin, A. A. (2011). *Acta Cryst.* D**67**, 355–367.
Nagase, H. & Woessner, J. F. Jr (1999). *J. Biol. Chem.* **274**, 21491–21494.
Ndinguri, M. W., Bhowmick, M., Tokmina-Roszyk, D., Robichaud, T. K. & Fields, G. B. (2012). *Molecules*, **17**, 14230–14248.

Neumann, U., Kubota, H., Frei, K., Ganu, V. & Leppert, D. (2004). *Anal. Biochem.* **328**, 166–173.
Pavlovsky, A. G., Williams, M. G., Ye, Q.-Z., Ortwine, D. F., Purchase, C. F. II, White, A. D., Dhanaraj, V., Roth, B. D., Johnson, L. L., Hupe, D. J., Humblet, C. & Blundell, T. L. (1999). *Protein Sci.* **8**, 1455–1462.
Tallant, C., Marrero, A. & Gomis-Rüth, F. X. (2010). *Biochim. Biophys. Acta*, **1803**, 20–28.
Udi, Y., Fragai, M., Grossman, M., Mitternacht, S., Arad-Yellin, R., Calderone, V., Melikian, M., Toccafondi, M., Berezovsky, I. N., Luchinat, C. & Sagi, I. (2013). *J. Mol. Biol.* **425**, 2330–2346.
Vagin, A. & Teplyakov, A. (2010). *Acta Cryst.* D**66**, 22–25.
Vargová, V., Pytliak, M. & Mechírová, V. (2012). *Matrix Metalloproteinase Inhibitors*, edited by S. P. Gupta, pp. 1–33. Basel: Springer.
Winn, M. D. *et al.* (2011). *Acta Cryst.* D**67**, 235–242.